THE JOURNAL OF PHYSICAL CHEMISTRY B LETTERS

2005, *109,* 17019−17024
Published on Web 08/19/2005

Systematic Coarse-Graining of Nanoparticle Interactions in Molecular Dynamics Simulation

Sergei Izvekov,[†] Angela Violi,[†,‡] and Gregory A. Voth*[,†]

Center for Biophysical Modeling and Simulation and Department of Chemistry, University of Utah, 315 S. 1400 E., Rm. 2020, Salt Lake City, Utah 84112-0850, and Department of Mechanical Engineering, University of Michigan, Ann Arbor, Michigan 48109

Received: June 7, 2005; In Final Form: July 30, 2005

A recently developed multiscale coarse-graining procedure [Izvekov, S.; Voth, G. A. *J. Phys. Chem. B* **2005**, *109*, 2469] is extended to derive coarse-grained models for nanoparticles. The methodology is applied to C_{60} and to carbonaceous nanoparticles produced in combustion environments. The coarse-graining of the interparticle force field is accomplished applying a force-matching procedure to data obtained from trajectories and forces from all-atom MD simulations. The CG models are shown to reproduce accurately the structural properties of the nanoparticle systems studied, while allowing for MD simulations of much larger self-assembled nanoparticle systems.

I. Introduction

To use molecular dynamics (MD) methods to simulate nanoparticle self-assembly, while at the same time to increase the time and length scales accessible in the simulations, it is necessary to describe the particles at a more coarse-grained (CG) level. In the past, a number of CG approaches have been proposed for macromolecular systems such as polymers or biomembranes.[1−12] The philosophy of these CG approaches is generally the same: to achieve a simpler description of the effective interactions in a given system while not losing the ability of the resulting models to predict the properties of interest.

The construction of CG models can be divided into two distinct phases: the first is the partitioning of the system into the larger CG structural units to reduce the system complexity, while the second is the construction of an effective force field to describe the interactions between the CG units. The latter stage is the most difficult and hampers the development of reliable CG models. In general, there has been no systematic multiscale strategy for the parametrization of such models. Typically, the CG potentials of a pre-selected analytical form are parametrized either to reproduce average structural properties seen in all-atom simulations, for example using an iterative adjustment of potential parameters starting from an approximation based on potentials of mean force[2,6,7] or the Inverse Monte Carlo technique,[8,12] or they are parametrized to match thermodynamic properties.[11] These approaches are not directly based on the underlying atomistic-scale forces, which are available from the atomistic-scale MD simulations.

Several factors contribute to the need for computationally efficient methods for the development of CG potentials. For instance, due to the poor transferability of the CG potentials across a range of thermodynamic conditions, the applicability of CG models, which are not as universal as their atomistic counterparts, is somewhat questionable. A CG simulation is therefore more reliable if the CG potentials are fit (or re-fit) to a system under the same thermodynamic conditions for which the system is intended to be simulated.

Caution must also be exercised with CG models as the dynamics are changed from the missing degrees of freedom and a softening of the interactions. As a result, the CG models may be unable to reproduce time correlation functions and, therefore, physical properties that rely upon them. For example, self-diffusion, which is defined by a time integral of a velocity−velocity time correlation function, might be wrong. Generally, in condensed-phase simulations, CG models show an accelerated dynamics because of the missing dissipation from the eliminated degrees of freedom. Ongoing work in our group will address this CG dynamics challenge, but it is not the focus of the present paper, which is the structural properties of self-assembled nanoparticles.

In the present paper, it is demonstrated that such a CG procedure is possible for nanoparticle systems based on our earlier work for biomolecular systems.[13] The present work represents an important new advance because nanoparticles are structurally dissimilar to biomolecules and they also interact through generally different and weaker interactions.

II. Methods

Recently, a force-matching (FM) method for obtaining the effective pairwise force fields for systems in condensed phases has been proposed.[14−16] More algorithmic details on this method are given in refs 13−17. The description of the FM method details relevant to the present work are given in Supporting Information.

Building upon this new FM methodology, a technique called "multi-scale coarse-graining" (MS−CG) has been developed,[13,17] which provides a systematic way for coarse-graining the interactions from the reference all-atom MD simulations. The

* Corresponding author.
[†] University of Utah.
[‡] University of Michigan.

10.1021/jp0530496 CCC: $30.25 © 2005 American Chemical Society

main idea of the MS−CG method is to apply the FM procedure to the CG images from underlying atomistic trajectory/force data. The most obvious way to map an atomic group into a CG site is to associate it with its center-of-mass (CM) because the force acting on the CM of the atomic group can be straightforwardly evaluated from the atomistic MD data. The FM procedure, when applied to these data, yields the effective interaction between the CG sites *as is present in the underlying all-atom simulation*. As an alternative, the CG site can coincide with the geometrical center of the structure (i.e., the CM of the system assuming that all atoms have the same mass). This is a more preferable choice for atomic groups with highly uneven mass distribution. As stated earlier, however, the coarse-graining of nanoparticle systems presents a special challenge for the MS−CG methodology because their shapes may be quite diverse, i.e., ranging from the highly symmetric C_{60} to more amorphous and irregular shapes such as in the carbon nanoparticles produced in combustion environments (soot precursors).[18,19] They also generally interact through the sum of many weaker interactions rather than via strong electrostatics in, e.g., an aqueous environment.

III. Applications

In the present work, we have applied the MS−CG method to obtain CG models of several carbonaceous nanoparticles, including those produced in flames.[18,19] Given the complexity of these combustion-produced systems, a complementary benchmark study has also been carried out for the C_{60} fullerene. Indeed, fullerenes are nanoscale carbon particles representative in some way of combustion-based nanoparticles, but with much higher symmetry. Specifically, they are in the same size range as the smallest nanoparticles and can aggregate to form larger clusters. Figure 1a depicts the all-atom structure of the C_{60} fullerene, while Figures 1b and 1c show two carbonaceous nanoparticles produced in flames.

A. C_{60} Nanoparticles. The force field describing the interactions between the CG sites in the C_{60} system was derived using the atomistic trajectory and the force data from a MD simulation of a system of 64 identical nanoparticles. The Lennard-Jones potential was used to describe the interatomic interactions with its parameters taken from ref 20. The geometry of particles was assumed to be rigid. The MD simulation was carried out in a 6.0 nm cubic supercell with periodic boundary conditions and the interactions were cutoff at 1.5 nm. The temperature of the system was kept constant at $T = 1600$ K, which represents a typical value of flame conditions. The high temperature also produces a better sampling (in a sense that it is more diverse) for the purpose of the FM procedure. The MD simulation was carried out in the constant NVT ensemble, and the trajectory and the force data were sampled at an interval of 0.05 ps. Then, these data were collapsed into trajectories and forces of the CG sites, and the resulting CG trajectory and force data were used as an input to the FM algorithm. The overdetermined system of linear FM equations was solved repeatedly for 12 000 sets of atomic configurations from 1.2 ns of MD trajectory data, with each set consisting of two configurations and then averaged over all sets. The force field was represented by a spline over a mesh with a grid spacing of approximately 0.0025 nm. The potentials were calculated by integrating out the respective terms in the force fields and then shifting them to zero at the cutoff radius. Although these manipulations might be viewed as a source of error in the simulated energetics, the way in which the potentials are calculated should not influence the behavior of the system in the MD simulations because in our framework

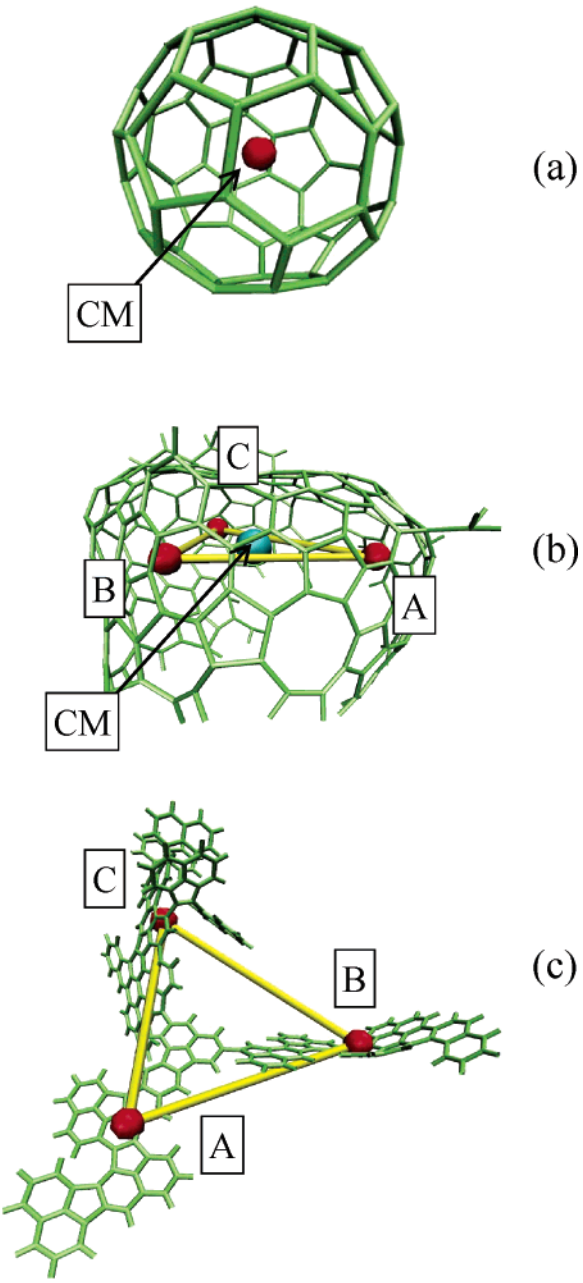


Figure 1. Atomistic and coarse-grained representations of C_{60} and two carbonaceous nanoparticles.

the FM forces are not derived from the potentials. More compact analytical representations of the FM force field, which are easier to implement, can be obtained by least-squares fitting the spline data using polynomial expansions that also smooth out roughness in the original force profiles.

The one-site CG model for C_{60} was parametrized with the CG interaction site placed at the center of mass of the molecule. The analytical representation of the resulting force field, as an expansion in powers of $1/r$ (which described in the caption to Table 1), is summarized in Table 1 and plotted in Figure 2a. The equilibrium spacing in $C_{60}-C_{60}$ dimer in vacuum from the CG model is 1.006 nm, with a well depth of −22.90 kJ/mol, which compares very favorably to the corresponding numbers from the atomistic dimer properties of 1.005 nm and −26.81 kJ/mol, respectively. The slight inconsistency in the equilibrium distance is within the bin size of the spline mesh. However, the vacuum MS−CG dimer binding energy is in worse agreement with the atomistic reference data. This is a consequence of the

TABLE 1: Coefficients A_n of the Least-Squares Fit of $C_{60}-C_{60}$ CG One-Site Force Field Using the Expansion in $f(r) = \sum_{n=2}^{16} A_n/r^n$ [a]

n	A_n
2	−6114.9880181854
3	1209886.4540479
4	−101315690.13431
5	4656062375.8825
6	−126807675441.53
7	2044573360846.6
8	−17993996887869
9	65114039870476
10	20439386000340
11	3605103615776.5
12	477358387546.85
13	52899207266.312
14	5185827122.3380
15	464738507.32768
16	38891390.925299

[a] Atomic units were used. The cutoff of up to 1.84 nm can be applied to this expansion.

condensed-phase force averaging over different particle orientations inherent in the MS−CG method. Indeed, the FM procedure approximates the potential of mean force acting on the CG site in the many-particle simulation. Because the CG force depends on the particular thermodynamic state of the system, it can deviate from the total zero-temperature gas-phase atomistic force acting on the dimer atomic group representing the CG site in the CG model. This deviation should be smaller if an atomic group to coarse-grain has a higher symmetry such as in C_{60}. Also, as mentioned above, the MS−CG models by FM are expected to be less transferable to other phases and thermodynamic conditions than their underlying all-atom models. The FM procedure needs to be repeated for each thermodynamic condition because it gives the derivative of the potential of mean force between CG sites, and this may vary with the thermodynamic conditions. This fact influences the accuracy of the present MS−CG models when compared to small clusters of particles at zero temperature in vacuum (e.g., a dimer) because the MS−CG models were derived from condensed-phase, many-particle simulations at a given thermodynamic temperature.

For the purpose of calculation of structural properties and making a comparison with the reference all-atom simulations, the MS−CG simulations were carried out for a system of 1024 C_{60} particles. These simulations were 10 ns long, preceded by about 5 ns of equilibration. However, much larger system sizes and longer time scales can be easily accessed, not only because in MS−CG models the number of sites is reduced but also because a much larger time step can be used in the integration of the CG system dynamics. For example, the one-site CG models of C_{60} nanoparticles can be integrated with time step of 0.1 ps, which is to be contrasted with the time step in all-atom MD simulation at 1600 K of 0.002 ps. As an example, for the CG model of C_{60}, in which the number of interactions centers reduced from sixty to one per C_{60}, nanoparticle, the computational efficiency for a system of 1024 particles is increased by $\sim 10^5$ times.

The CG model of C_{60} is able to reproduce the structural properties of the system as is shown in Figure 3a, where the CG site−site radial distribution functions (RDFs) from CG and all-atom MD simulations are compared. The overall agreement is very good. The only meaningful difference is a decrease in the first peak height obtained with the atomistic MD run compared with the one from the MS−CG simulation. However, this could instead be due to equilibration issues, since the CG system was much larger in size and simulated for much longer times than the one used for the atomistic MD runs. Previous attempts to develop a one-site model for the C_{60} molecule[21,20] were based on a treatment of the C_{60} molecules as if they were perfect spheres and averaging the potential over their surfaces.

B. Carbonaceous Nanoparticles from Combustion Sources. As a second application, we analyzed carbonaceous nanoparticles produced in aromatic and aliphatic flames, whose structures were obtained using a combination of kinetic Monte Carlo (KMC) and molecular dynamics (MD) methodologies (The Atomistic Model for Particle Inception, or AMPI, code). The AMPI code[18,19] has been developed to study the transformations that occur in combustion systems during the transition from gas phase to particle inception. Figures 1b and 1c show two representative structures obtained in a benzene and an acetylene flame, respectively. The reaction pathways for the growth of incipient particles depend on the fuel. In the case of aromatic fuels, polymerization reactions can occur early since aromatic compounds, such as benzene and naphthalene, are in relatively large concentrations. By contrast, in the case of aliphatic fuels, such as acetylene or ethylene, the first aromatic ring must be formed from fuel decomposition products by a sequence of elementary reactions and therefore in the inception region the concentrations of polycyclic aromatic precursors are lower than in the aromatic flame. These considerations explain the different morphologies of the particles produced in the two environments. The nanoparticle produced in the benzene flame ($C_{189}H_{35}$ "round') has an aspect ratio much lower than the one obtained in the aliphatic flame ($C_{202}H_{90}$ "flat"). The first particle has a bowl-like shape with an opening directed downward in Figure 1b. All dangling bonds of carbon atoms have been hydrogen terminated.

To build the CG system for the round and flat nanoparticles, atomistic MD simulations were carried out on two systems: the first one was composed of 64 identical round particles (Figure 1b) and the second made of 64 identical flat particles (Figure 1c). For the interactions between nanoparticles, the CHARMM force field parameters[22] were used. The sizes of the supercells used for the round and flat particles were 7 and 12 nm, respectively, and the interaction cutoff was set at 1.75 nm. The temperature, the time step to integrate the particle's dynamics, the length of the simulations, and the sampling of data for the FM procedure were the same as those used for the C_{60} system. Since these nanoparticles have a much more complex geometry than the C_{60}, the spline data representing FM force fields were refitted using a Chebyshev series,[23] as explained in ref 16 because of its faster convergence. The coefficients of Chebyshev expansions for both nanoparticle geometries are given in the Supporting Information and can be used to implement the models.

A one-site CG model, which has the site located on the CM of the nanoparticle (cf. Figure 1b), was first developed for the round particle and the computed FM force and potential are reported in Figure 2b. The error bars for the matched CG forces are shown at the representative distances. Larger errors for smaller separations are a reflection of the fact that fewer configurations sampled the respective spline mesh bins. The effective force profile shows a complex structure up to a separation of 1.7 nm, which is close to the largest intraparticle separation. Variations with distance in the effective CG force field are partially due to a change in the average availability of different mutual orientations of the nanoparticles. For example, two nanoparticles could reach small separations between their CMs only if they directed to each other by sides opposite to their openings (see Figure 1b). Some features in the force profile

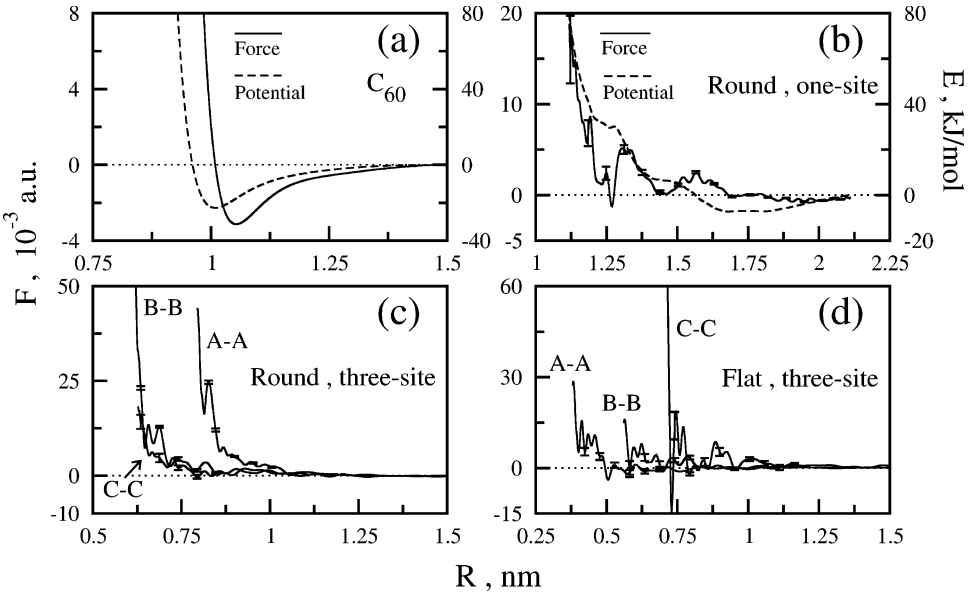


Figure 2. Effective pairwise forces and potentials for MS−CG models of C_{60} and carbonaceous nanoparticles as functions of intersite separation calculated by the force-matching method. Panel (a): One-site model of C_{60}. Panel (b): One-site and three-site models of round particle. Panel (c): Three-site model of flat particle.

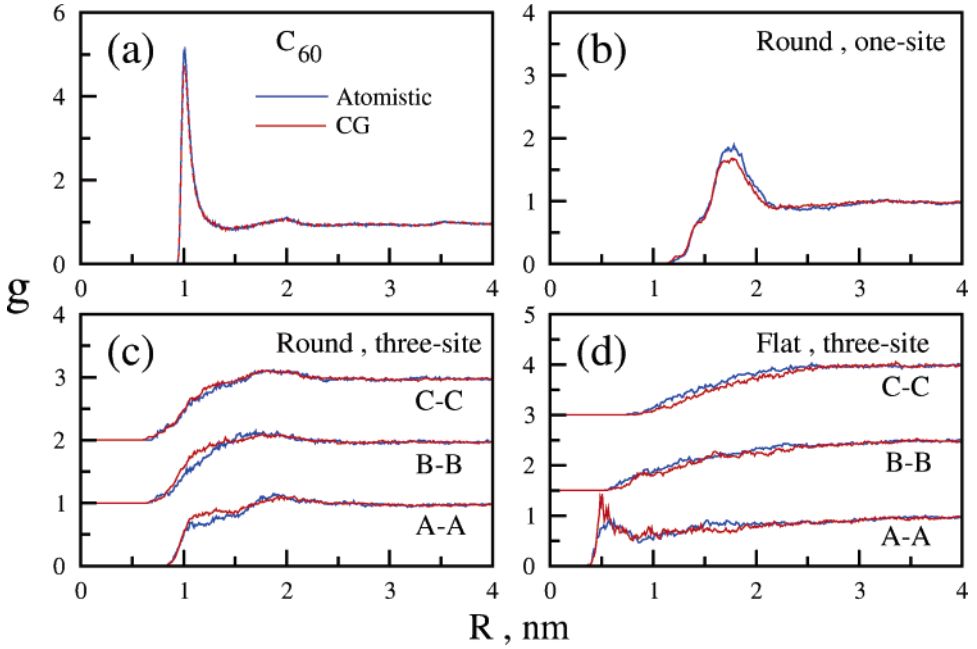
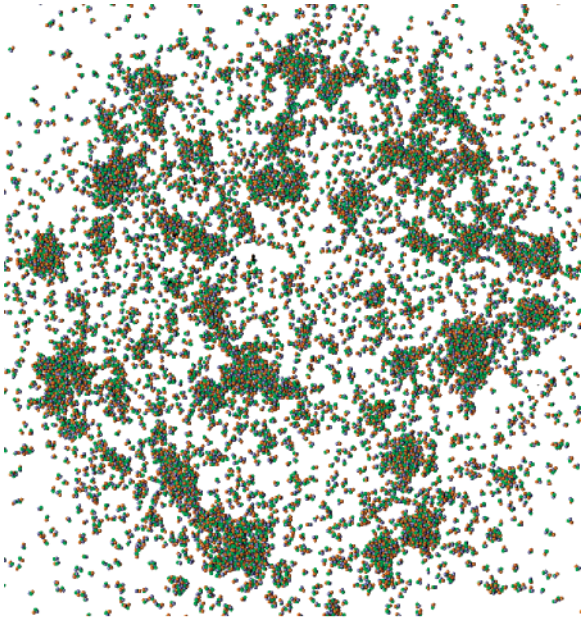


Figure 3. Selected site−site RDFs from underlying atomistic MD simulation (blue lines) compared to those from MS−CG MD simulation (red lines) for the various systems.

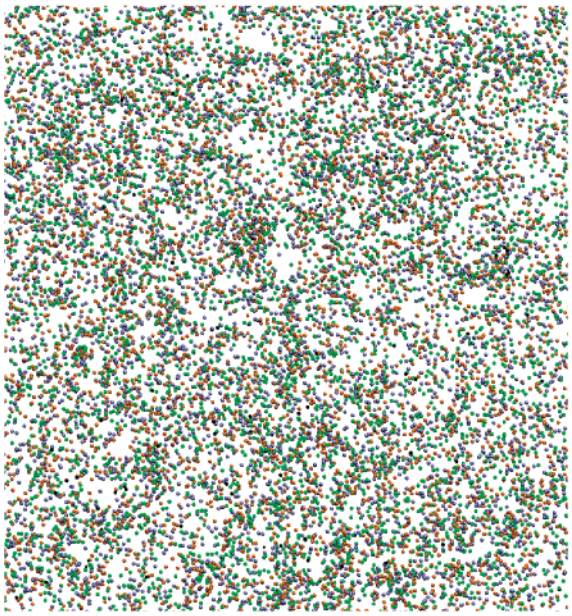
result in very shallow minima in the potential and are likely irrelevant for the simulated properties as they compete with thermal fluctuations. However, as seen from the error bars, the humps and dips in the force profile are likely not statistical noise. The effective interaction is attractive beyond 1.68 nm, suggesting significant aggregation tendencies for the bowl-like nanoparticles, even at high temperature (see later results).

The structural properties extracted from the MS−CG MD simulation of the many-particle system agree well with their atomistic counterparts as demonstrated in Figure 3b. Dips in the force around 1.27 nm (when the force is negative) and 1.45 nm (when force is almost zero) are likely responsible for the formation of steps in the front slope of the first peak of the CM-CM distribution function. The well pronounced first peak is due to the attractive part of the effective potential which has a depth of −7.1 kJ/mol and is centered around 1.75 nm. The agreement in the structural properties is an important result since it reveals that even a simple MS−CG model with one interaction site is able to reproduce accurately the structural properties for a system of particles having such a large size and complex geometry. Similar to the C_{60} system, the deviation in the magnitude of the first maximum of the RDFs between the CG and the all-atom simulations might be explained by the different degree of equilibration reached in both simulations.

To study more complex processes, such as the self-assembly or the structural transitions of nanoparticles, the one-site model is not a proper choice since it does not account for orientational degrees of freedom of the particles. The obvious solution is a CG model with several additional interaction sites. For example, a three-site CG geometry may be considered as a clear improvement, as this CG system adds orientational degrees of freedom into the model. Here we describe the three-site CG



(a)



(b)

Figure 4. Snapshots from CG MD simulations using three-site CG models of round [Panel (a)] and flat [Panel (b)] nanoparticles at 1000 K. The CG modes were fitted to all-atom MD simulations at same temperature. Effectively ~2 million atoms are simulated for 500 ns in these results, yield very different mesoscopic aggregation behavior.

models developed for both the round and flat nanoparticles. The round nanoparticle was mapped into a three-site geometry by slicing it into three segments of approximately equal weight by planes perpendicular to the opening plane of the particle. The CG interaction sites were associated with the CM of the corresponding segments as shown in Figure 1b (sites A, B and C). The same trajectories and forces that were utilized to construct the one-site model were collated into trajectories and forces of the new CG sites, and then the FM procedure was applied to obtain the effective CG force field. The resulting force profiles for selected pairs of CG sites, after being smoothed out using a polynomial fit which is presented in the Supporting Information, are shown in Figure 2c. A comparison of the RDFs obtained from the MS−CG and the all-atom MD simulations are given in Figure 3c. The agreement is again seen to be very good.

Similar to the round particle, the flat nanoparticle was divided into three segments in accordance to its three "wings". The CG sites were associated with the CM of the corresponding segments as shown in Figure 1c (sites A, B and C). The FM procedure was then similar to the one applied to the round particle. Selected smoothed force profiles are depicted in Figure 2d, and the analytical representation is given in the Supporting Information. The comparison of the structural properties from the MS−CG and all-atom MD simulations is given in Figure 3d, with a general level of agreement comparable to the previous cases. A well-pronounced first peak in the A−A RDF reflects an attractive character of the interaction between A sites at this separation that can be seen from an inspection of the force profile in Figure 2.

A further application of the MS−CG models was to study the combustion-generated nanoparticle aggregation behavior at lower temperatures. We therefore reparametrized the CG force fields for both the round and flat geometries using all-atom MD simulations at 1000 K and at higher density by approximately three times compared to the 1600 K case. The CG MD simulations were then conducted on a system of 10 000 CG particles (or effectively ~2 million atoms) for 500 ns. The simulations were initiated from energy minimized (blob-like) configurations. Figure 4 shows snapshots from the end points of these two simulations. The system of round nanoparticles clearly exhibits the presence of clusters which were observed to persist for the entire length of the simulation. By contrast, the system of flat particles does not manifest long-lived aggregates of any kind. The combined magnitude of this simulation on both size and time would be very difficult, if not impossible at the present time, to achieve in an all-atom MD simulation. The MS−CG models developed here can be thus seen as prototypes of more realistic models to study complex aggregation phenomena during the nanoparticle self-assembly process.

Concluding Remarks

In conclusion, the recently developed MS−CG method[13,17] for obtaining effective pairwise CG force fields from atomistic force and trajectory data has been shown here to be very successful in developing CG models for systems of nanoparticles. This approach in principle provides a connection between the various time and length scales in the nanoparticle self-assembly problem, together with an unprecedented opportunity for the understanding of the atomistic interactions underlying nanoparticle aggregation and self-assembly. In the future, the MS−CG approach can be straightforwardly applied to nanoparticle systems containing a variety of geometries. The obvious complication will be an increase in the number of CG interaction sites of different types (i.e., a larger number of species found in a CG representation of the system). As an example, for carbonaceous nanoparticles higher resolution MS−CG models can be developed by coarse-graining the subnanometer PAHs that represent the precursors of the carbonaceous nanoparticle agglomerates. The resulting MS−CG models can then be used, e.g., to simulate the primary soot particle formation. The new MS−CG models of nanoparticles may also allow us to also study the phase transitions to orientational alignment of the bigger carbonaceous primary particles, which are likely responsible for the experimentally observed structures of carbonaceous clusters found in combustion and other important environments.

Additional applications of the MS−CG method for nanoparticle self-assembly are also clearly possible.

Acknowledgment. This research is funded by a National Science Foundation Nanoscale Interdisciplinary Research Team grant (EEC-0304433) and the University of Utah Center for the Simulation of Accidental Fires and Explosions (C-SAFE), funded by the Department of Energy, Lawrence Livermore National Laboratory, under subcontract B341493.

Supporting Information Available: Details of the force-matching algorithm and coefficients of the least-squares fits of CG force fields for round and flat nanoparticles using the expansion in a Chebyshev series. This material is available free of charge via the Internet at http://pubs.acs.org.

References and Notes

(1) Smit, B.; Esselink, K.; Hilbers, P. A. J.; van Os, N. M.; Rupert, L. A. M.; Szleifer, I. *Langmuir* **1993**, *9*, 9.
(2) Head-Gordon, T.; Stillinger, F. H. *J. Chem. Phys.* **1993**, *98*, 3313.
(3) Palmer, B. J.; Liu, J. *Langmuir* **1996**, *12*, 746.
(4) Goetz, R.; Lipowsky, R. J. *J. Chem. Phys.* **1998**, *108*, 7397.
(5) Shelley, J. C.; Shelley, M. Y. *Curr. Opin. Colloid Interface Sci.* **2000**, *5*, 101.
(6) Meyer, H.; Biermann, O.; Faller, R.; Reith, D.; Müller-Plathe, F. *J. Chem. Phys.* **2000**, *113*, 6264.
(7) Shelley, J. C.; Shelley, M. Y.; Reeder, R. C.; Bandyopadhyay, S.; Klein, M. L. *J. Phys. Chem. B* **2001**, *105*, 4464.
(8) Garde, S.; Ashbaugh, H. S. *J. Chem. Phys.* **2001**, *115*, 977.
(9) Marrink, S.; Mark, A. *J. Am. Chem. Soc.* **2003**, *125*, 15233.
(10) Stevens, M. J.; Hoh, J. H.; Woolf, T. B. *Phys. Rev. Lett.* **2003**, *91*, 188102.
(11) Marrink, S. J.; de Vries, A. H.; Mark, A. E. *J. Phys. Chem. B* **2004**, *108*, 750.
(12) Murtola, T.; Falck, E.; Patra, M.; Karttunen, M.; Vattulainena, I. *J. Chem. Phys.* **2004**, *121*, 9156.
(13) Izvekov, S.; Voth, G. A. *J. Phys. Chem. B* **2005**, *109*, 2469.
(14) Izvekov, S.; Parrinello, M.; Burnham, C. J.; Voth, G. A. *J. Chem. Phys.* **2004**, *120*, 10896.
(15) Hone, T. D.; Izvekov, S.; Voth, G. A. *J. Chem. Phys.* **2005**, *122*, 54105.
(16) Izvekov, S.; Voth, G. A. *J. Phys. Chem. B* **2005**, *109*, 6573.
(17) Izvekov, S.; Voth, G. A. *J. Chem. Phys.* **2005**, in press.
(18) Violi, A.; Sarofim, A. F.; Voth, G. A. *Comb. Sci. Technol.* **2004**, *176*, 991.
(19) Violi, A. *Combust. Flame* **2004**, *139*, 279.
(20) Girifalco, L. A.; Hodak, M.; Lee, R. *Phys. Rev. B* **2000**, *62*, 13104.
(21) Girifalco, L. A. *J. Phys. Chem.* **1992**, *96*, 858.
(22) Brooks, B. R.; Bruccoleri, R. E.; Olafson, B. D.; States, D. J.; Swaminathan, S.; Karplus, M. *J. Comput. Chem.* **1983**, *4*, 187.
(23) Rivlin, T. J. *Chebyshev Polynomials;* Wiley: New York, 1990.